

# RETURN TO MERCURY: AN OVERVIEW OF THE MESSENGER SPACECRAFT THERMAL CONTROL SYSTEM DESIGN AND UPDATE ON ORBITAL FLIGHT PERFORMANCE

Carl J. Ercol,<sup>1</sup> Shawn M. Begley,<sup>2</sup> and G. Allan Holtzman<sup>3</sup>

At 01:00 UTC on March 18, 2011, the MErcury Surface, Space ENvironment, GEochemistry, and Ranging (MESSENGER) spacecraft became the first to achieve orbit around the planet Mercury. Designed and built by The Johns Hopkins University Applied Physics Laboratory in conjunction with the Carnegie Institution of Washington, MESSENGER was launched on August 3, 2004, and has recently completed its primary mission of a one-year orbital phase to study Mercury. Currently, MESSENGER is in the initial portion of a yearlong extended mission to gather more science with an orbit period that was shortened from 12 to 8 hours. Before orbit injection at Mercury, the spacecraft completed a seven-year cruise phase that included a flyby of the Earth (August 2005), two flybys of Venus (October 2006 and June 2007), and three flybys of Mercury (January and October 2008 and October 2009). The January 2008 Mercury flyby marked the first spacecraft visit to Mercury since Mariner 10 (1975) and made MESSENGER the first spacecraft to encounter Mercury near the planet's perihelion. This paper will provide an overview of the thermal design challenges for both the cruise and orbital phases and the flight temperature and power data that verify the performance of the mission thermal control subsystem to date.

## INTRODUCTION

The MErcury Surface, Space ENvironment, GEochemistry, and Ranging (MESSENGER) mission has been characterizing Mercury in detail by observing the planet from orbit for one Earth year. Although it had long been desired to follow the Mariner 10 flybys with an orbital mission, early studies had deemed this type of mission infeasible, or at least prohibitively expensive because of mass and thermal constraints. MESSENGER utilized a trajectory, discovered by analysts at the Jet Propulsion Laboratory (JPL) [1, 2] and later refined by analysts at The Johns Hopkins University Applied Physics Laboratory (APL), in which flybys of Earth, Venus, and Mercury itself, interspersed with five large deterministic deep-space maneuvers (DSMs), positioned the spacecraft for its successful Mercury orbit insertion (MOI) on March 18, 2011 (see Figure 1).

---

<sup>1</sup>Thermal Design and Operations Lead Engineer, The Johns Hopkins University Applied Physics Laboratory, 11100 Johns Hopkins Road, Laurel, MD 20723.

<sup>2</sup>Instrument Operations and Analysis Thermal Lead, The Johns Hopkins University Applied Physics Laboratory, 11100 Johns Hopkins Road, Laurel, MD 20723.

<sup>3</sup>Spacecraft Analysis and Operations Thermal Lead, The Johns Hopkins University Applied Physics Laboratory, 11100 Johns Hopkins Road, Laurel, MD 20723.

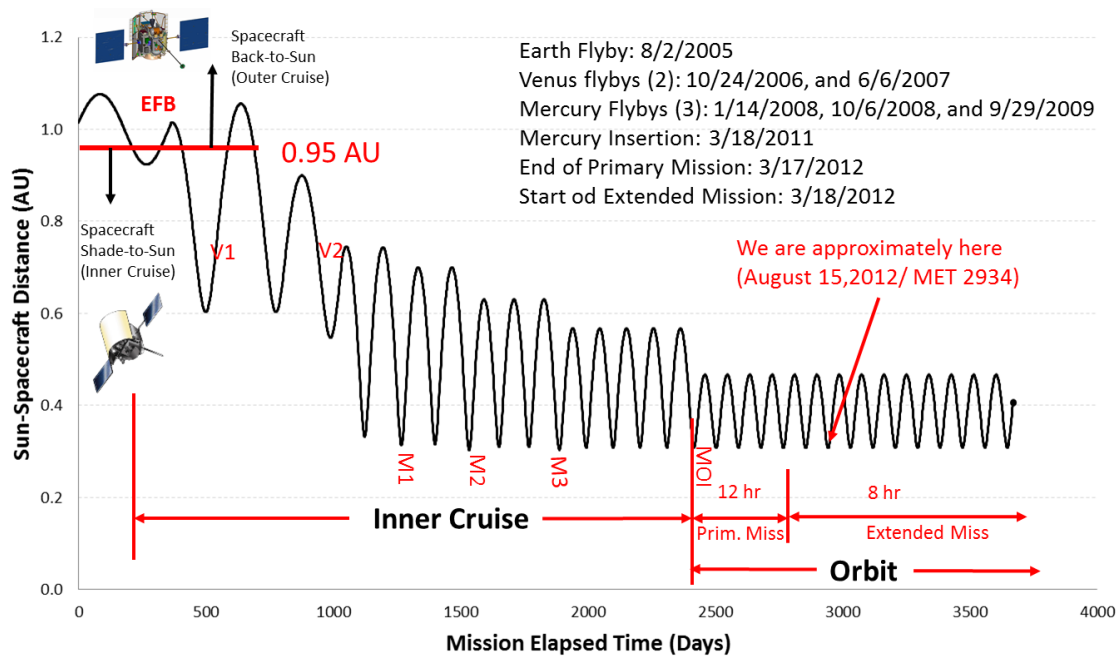


**Figure 1. Shown is the variation in spacecraft-to-Sun distance as a function of elapsed mission day during the MESSENGER mission. Key mission events are highlighted. Currently, MESSENGER is approximately at the midpoint of its first extended orbit mission. EFB, Earth flyby; M1–M3, Mercury flybys 1–3; MET, mission elapsed time; V1 and V2, Venus flybys 1 and 2.**

The highly varying thermal environments expected during the cruise and Mercury orbital phases were a key engineering challenge in the spacecraft design. Driven by solar distances as small as 0.30 AU, the spacecraft thermal protection is accomplished with a large sunshade that shields most spacecraft components from direct solar exposure and allows them to operate at conditions typical of other interplanetary spacecraft. The orbital geometry as a function of Mercury true anomaly (MTA) was chosen via comprehensive thermal environment analysis to minimize the thermal hazards on the dayside of Mercury [3] by factoring analytical thermal constraints into the mission design. While in orbit, MESSENGER experiences steady-state heating from the Sun and transient heating from Mercury, both of which are functions of Mercury’s solar distance, which varies between 0.3 AU (perihelion) and 0.46 AU (aphelion). Because most of the spacecraft hardware is protected by the sunshade, no specialized thermal designs were required. Certain hardware (the solar panels, sunshade, phased-array and low-gain antennas, and Digital Sun Sensor [DSS] heads) is continuously exposed to the Sun throughout the mission and was specially designed to handle the temperatures and solar flux input experienced at 0.3 AU [4–7].

The MESSENGER mission is a collaboration between the Carnegie Institution of Washington (CIW) and APL and was selected as the seventh mission in NASA’s Discovery Program, with a formal project start in January 2000. The spacecraft engineering and science instrument design evolved over the three-year period from January 2000 to spring 2003. Assembly and integration of the spacecraft began in February 2003, and testing continued up to launch in August 2004. Orbital operations are now supported from the Mission Operations Center at APL with communications through NASA’s Deep-Space Network (DSN) antennas.

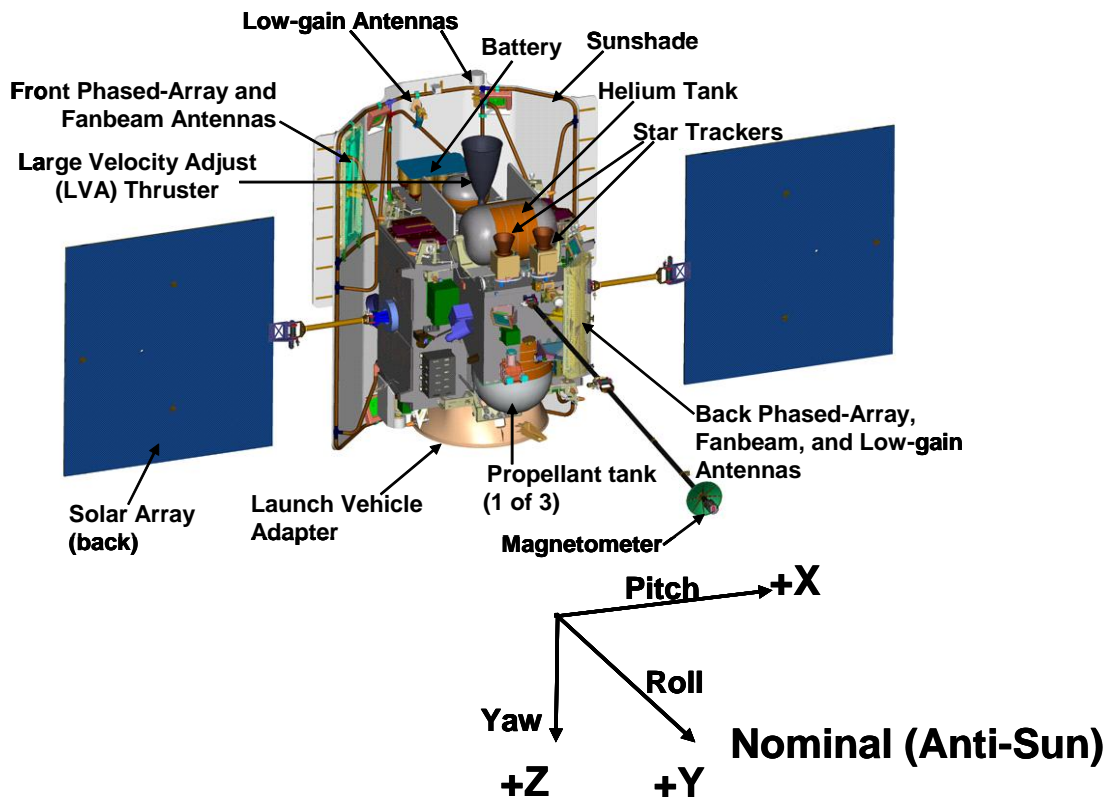


Figure 2. The MESSENGER spacecraft and flight coordinate system.

## OVERVIEW OF SPACECRAFT THERMAL DESIGN

The thermal design and operation of the MESSENGER spacecraft addressed three mission phases: outer cruise, inner cruise, and Mercury orbit. During the inner cruise and orbital phases, the thermal design relies on a ceramic-cloth sunshade to protect the vehicle from the intense solar environment encountered when inside of 0.95 AU. As shown in Figure 2, the sunshade creates a benign thermal environment when oriented with the  $-Y$  axis pointed toward the Sun, allowing for the use of standard electronics and electrical components and thermal blanketing materials. The solar arrays, sunshade, DSSs, and phased-array antennas, which are shown in Figures 3 and 4, are Sun-exposed components that required nonstandard thermal design and specialized construction. These components have been designed to operate throughout the Mercury year and also during orbits that cross over one of Mercury's two "hot poles" that face the Sun at Mercury perihelion. When at spacecraft perihelion, the sunshade, solar arrays, sunshade-mounted DSSs, and sunshade-mounted antenna suite experience as much as 11 times the solar radiation near Earth. During this time, the sunshade temperature rises to greater than 300°C. In certain orbits around Mercury, the spacecraft passes between the Sun and the illuminated planet for ~30 minutes. During this period, the sunshade protects the spacecraft from direct solar illumination, but the back of the spacecraft is exposed to the hot Mercury surface. Components such as the battery and star trackers are positioned such that the spacecraft body blocks a substantial portion of the planet view, minimizing direct radiation from the planet surface when the spacecraft is in nominal operation. High-power spacecraft electronics that require dedicated radiators could not be packaged in a manner similar to that of the battery to reduce environmental heating from Mercury. These electronics boxes instead required specialized thermal design to allow for full, unrestricted operation during all parts of the orbital

mission phase. Diode heat pipes, which are shown in Figure 5, were used in both the spacecraft and imager thermal designs to protect the attached components when radiator surfaces are exposed to dayside heating from Mercury. Thermal model results illustrating the variation of Mercury-induced heating received by MESSENGER are shown in Figure 6. During this peak heating period, the diode heat pipes effectively stop conducting when the radiator surface becomes hot, as simulated during spacecraft-level thermal vacuum testing and demonstrated in orbit with flight data in Figure 7. Once the planetary heating decays and the radiators begin to cool, the heat pipes resume conduction, restoring normal thermal control. Analysis of the near-planet environment as a function of orbit geometry and planet position was integrated into the mission design and has helped to phase the orbit plane relative to solar distance, minimizing infrared (IR) heating of the spacecraft by the planet and thus minimizing the mass required to accommodate such heating.

From launch until June 2006, there were three prolonged periods (see Figure 1) when the mission trajectory achieved solar distances  $>0.95$  AU and the MESSENGER spacecraft was flown in the reverse-sunshade orientation. This flight configuration allowed for select illumination of the spacecraft body that reduced heater-power usage to nearly zero and allowed for large power margins while maintaining component temperatures within their allowable flight limits. This capability also allowed MESSENGER to operate easily between 0.95 and 1.08 AU and gave unconstrained flexibility on outer solar distance when the mission design team was planning for backup



**Figure 3.** Shown is the MESSENGER spacecraft 2 weeks before launch. Highlighted here are the ceramic-cloth sunshade, the four DSSs with attenuating filters, the phased arrays and low-gain antennas under high-temperature radomes, and the 4.4-N pro-Sun thrusters.

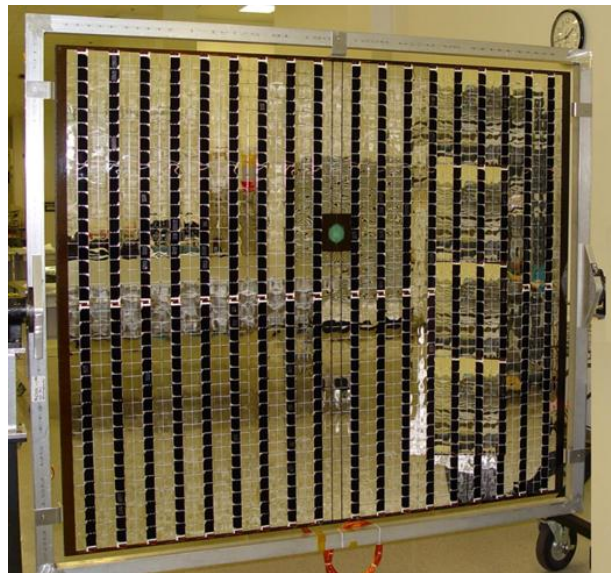


**Figure 4.** Shown here is the MESSENGER +X solar array before spacecraft integration. Each solar array has a 2:1 ratio of OSRs to triple-junction gallium-arsenide solar cells.

missions that introduced different mission trajectories and outer solar-distance excursions without complicating the spacecraft thermal or power designs. To achieve acceptable temperature control, spacecraft radiator surfaces used to maintain temperature for the battery and other critical electrical components were always kept orthogonal to the Sun, while ~25% of the spacecraft multi-layer insulation (MLI), the helium tank, and most of the thrusters were fully illuminated. Because this flight configuration was designed exclusively to minimize the effects of solar distance on the spacecraft power and thermal subsystem designs, certain operational constraints were enforced to prevent temperature excursions above the allowable flight limits for some components. Steady-state Sun elevation and yaw angles were limited to a  $\pm 5^\circ$  cone centered along the spacecraft +Y axis (the principal axis corresponding to the Magnetometer boom) so as to reduce solar exposure of spacecraft radiators and mitigate solar trapping inside of the adapter and the star tracker baffles. Because of the high thermal time constant for the spacecraft, transient events of less than 2 hours requiring Sun angle excursions outside of the  $\pm 5^\circ$  cone were acceptable and allowed for complete flexibility when performing spacecraft propulsive maneuvers, certain instrument calibrations, and post-launch hardware-commissioning activities.

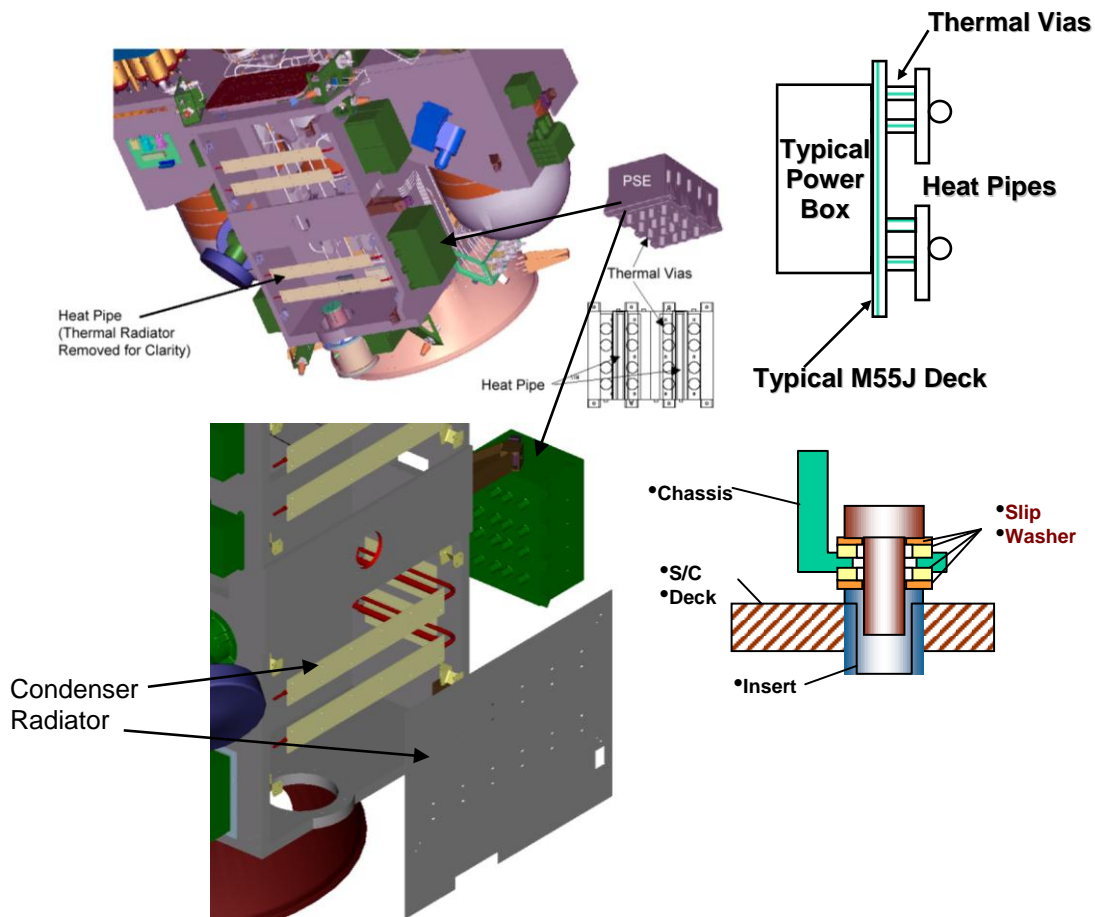


**Figure 5. Diode heat pipes were used to protect high-power electronics requirements during the Mercury orbit phase. The PSE, shown here, required dedicated radiators. Because the MESSENGER structure was fabricated from a composite with a small coefficient of thermal expansion, a slip-mount design was used to fasten electronics boxes to the structure, and integral thermal vias connect specified electronics boxes directly to the heat pipes. S/C, spacecraft.**

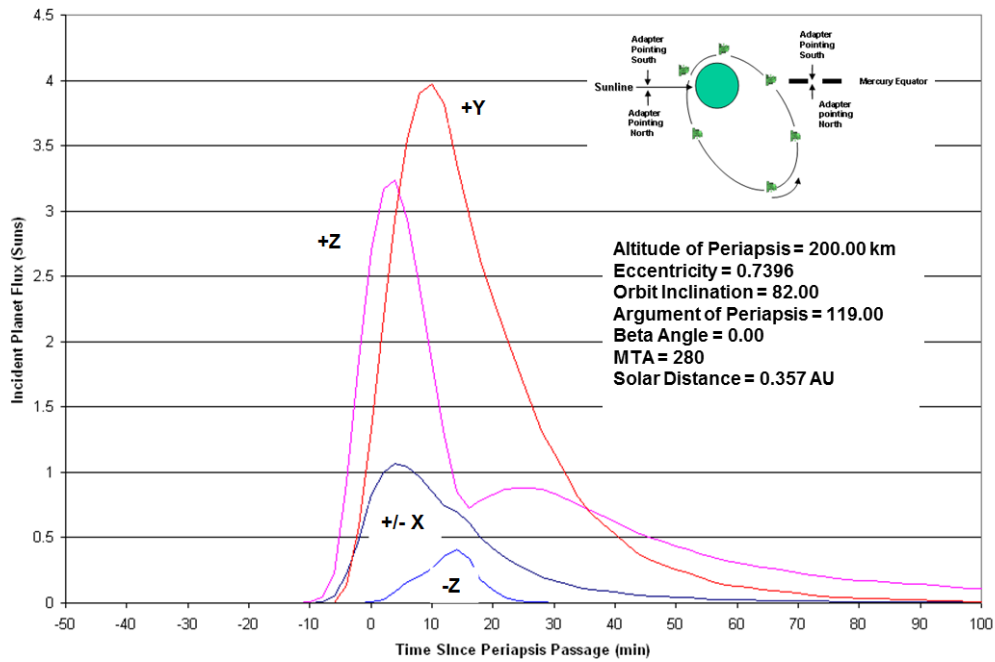


Figure 6. Shown is the predicted incident thermal flux emitted by Mercury as seen at different locations on the spacecraft. Spacecraft thermal-control radiators are located in the  $-Z$  and  $\pm X$  directions.

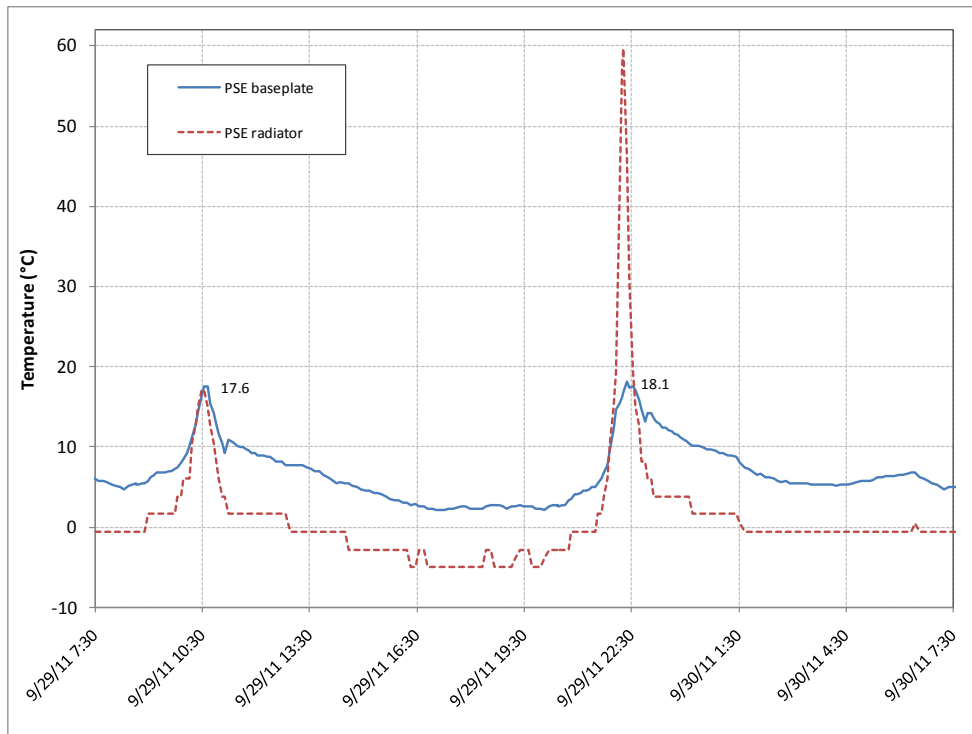
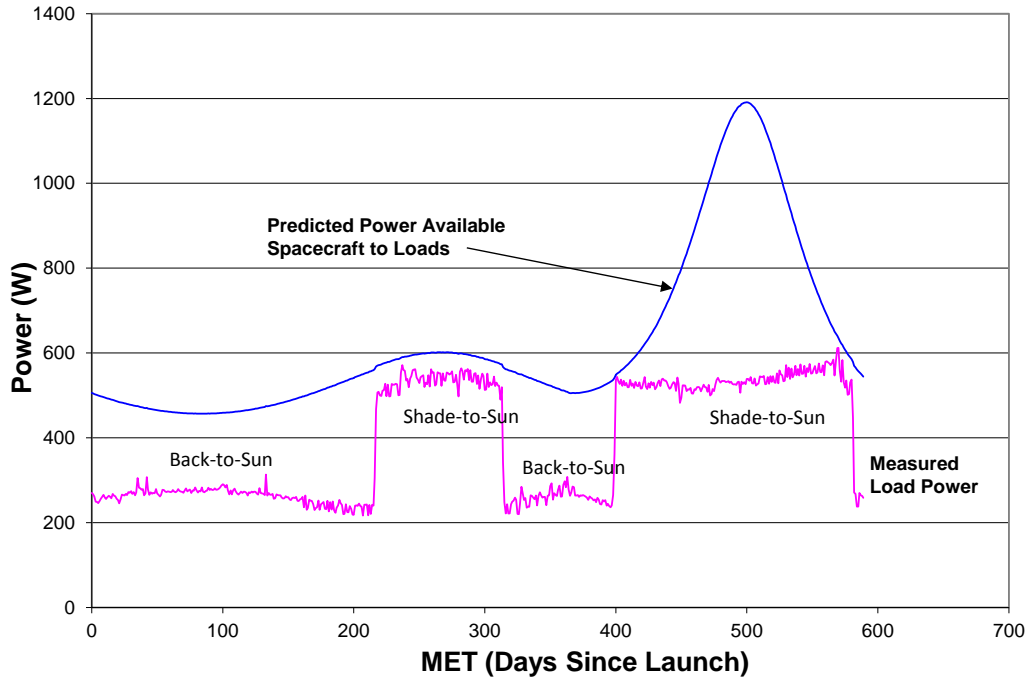


Figure 7. Shown is the PSE orbital temperature response during the first hot season of Mercury year three. The planetary heating on the PSE radiator increased sharply near September 29, 2011, at 10:30 UTC, causing the diode heat pipes to shut down and keeping the PSE comfortably cool.

Once power margins were deemed to be acceptable, the inner cruise phase began on March 8, 2005, when MESSENGER was transitioned into the nominal sunshade-to-Sun orientation from the reverse-sunshade orientation that had been maintained since launch. It was apparent within the first 24 hours from the transition that the sunshade was extremely effective at insulating the spacecraft from the Sun. The nominal spacecraft power of  $\sim 220$  W that was experienced when in the reverse-sunshade configuration more than doubled as dormant heaters became active (as shown in Figure 8). MESSENGER relies on heater power to keep components within allowable flight temperature limits, and because approximately one-half of spacecraft launch mass was propellant, the biggest user of heater power was the propulsion system.



**Figure 8. Power lean near Earth’s solar distance, the MESSENGER spacecraft was designed to be maneuvered so as to illuminate the spacecraft body, represented by the back-to-Sun label, as a means to reduce heater-power demand. When the power margin was adequate, the spacecraft was maneuvered into the shade-to-Sun (nominal flight attitude) orientation. As shown, the power difference between the two Sun orientations was  $\sim 220$  W. MET, mission elapsed time.**

Battery temperature control relies on two redundant heater circuits that are independently controlled by single mechanical thermostats. Heater control is augmented with 5 W of internal heat dissipation resulting from the constant trickle charge rate that maintains the battery at 100% state of charge. During reverse-sunshade orientation when the spacecraft was near 1.0 AU, the battery was maintained at less than  $0^{\circ}\text{C}$  with trickle charge and a small amount of heater power. When the spacecraft was flipped and the sunshade was oriented toward the Sun, the battery temperature was maintained at a nearly constant temperature of approximately  $-5^{\circ}\text{C}$  with 32 W of heater power and 5 W of trickle charge. As the solar distance decreased from near 1.0 AU to 0.63 AU, battery temperature increased from  $-5^{\circ}\text{C}$  to approximately  $-1^{\circ}\text{C}$  with the primary heater at 100% duty cycle. Once inside of 0.63 AU, the battery temperature cycled between  $-5^{\circ}\text{C}$  and  $-1^{\circ}\text{C}$  with the duty cycle varying as a function of solar distance (Table 1). To date, including more than five Mercury years in orbit, the MESSENGER battery has been maintained below

15°C. Peak battery heating occurs during the eclipsing noon–midnight orbital conditions when the spacecraft passes between the Sun and the planet.

**Table 1. Duty cycle variation in relation to solar distance**

Solar Distance (AU)	Heater Duty Cycle (%)
>0.65	100
0.63	93
0.56	89
0.50	81
0.42	70
0.39	51
0.31	34

*During inner cruise, the battery-heater duty cycle is affected by sunshade frontal temperature, which is a function of solar distance. When the spacecraft was flown in the reverse-sunshade orientation during outer cruise, the battery-heater duty cycle averaged between 0% and 20%.*

Mounted on the sunshade frame are four DSSs, three low-gain antennas, and the combined phased-array and fan-beam antenna assembly. To provide the spacecraft with hemispherical and directional antenna coverage along with a Sun-safe attitude determination, these components view the Sun continuously and were thermally designed and tested to meet all operational requirements when near the Earth and when at Mercury perihelion. The temperatures of these components as functions of solar distance are shown in Figure 9. It can be seen that the temperature increase of each component follows an inverse-squared-distance law.

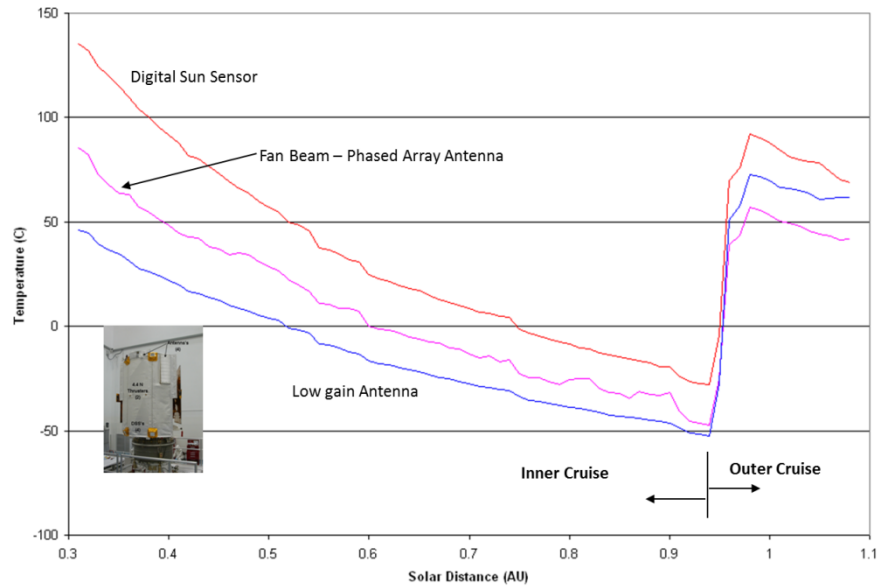


**Figure 9. The sunshade-mounted components (see Figure 3) behaved nominally as solar distance decreased. Comprehensive solar-simulation testing at the NASA Glenn Research Center (GRC) Tank 6 facility ensured that these components were designed to operate properly in MESSENGER’s high-solar-flux environment without any surprises.**

As with the sunshade-mounted components, the solar arrays always receive direct illumination from the Sun and had to be designed to operate and survive over a very broad range of



environments. Thermal control of the solar arrays is managed by using a 2:1 packing factor ratio of optical solar reflectors (OSRs) to triple-junction gallium-arsenide solar cells (Figure 4) combined with an ability to rotate each solar array independently. The off-normal tilting reduces the effective solar constant in proportion to the cosine of the angle of incidence. The thermal design of each panel, and hence the design driver for packing factor, allows for steady-state survivability at any Sun angle at any mission solar distance. Solar-array operation is discussed in more detail below.

The spacecraft electronics are mounted to the composite structure and, except for radiators and apertures, are completely covered with MLI. Complete spacecraft coverage with MLI, although attractive from the perspectives of heater power and coupled thermal mass, was not feasible, so electronics boxes dissipating, on average, greater than 20 W have dedicated radiators. These radiators effectively keep the connected electronics boxes cool and, in conjunction with MLI heat leakage, help to keep the rest of the spacecraft at benign temperatures. The Power System Electronics (PSE) and Inertial Measurement Unit (IMU) are located on the  $-X$  side of the spacecraft, and the two Integrated Electronic Modules (IEMs), the Power Distribution Unit (PDU), and the Solar Array Junction Box (SAJB) are located on the  $+X$  side of the spacecraft. The  $\pm X$ -side-panel radiator components increase the temperature by  $\sim 10^\circ\text{C}$ , as a result of thermal coupling to the solar arrays, as the solar flux changes by one order of magnitude. The Advanced Star Tracker (AST), located on the  $-Z$  deck, is unaffected by solar distance. Because the propulsion tanks are always under positive heater control, the heater duty cycle decreases as solar distance decreases and/or spacecraft electronics dissipation increases, keeping the main fuel tanks at nearly constant temperature. Because thermal performance of the MESSENGER spacecraft during inner and outer cruise phase has been comprehensively summarized [8–12], the remainder of this paper will focus on the orbital phase of the mission.

## **ORBITAL ENVIRONMENTS OVERVIEW**

Mercury's highly eccentric 88-day heliocentric orbit causes the solar flux to vary between 4.7 suns (planet aphelion, 0.46 AU) and 11.1 suns (planet perihelion, 0.30 AU), where one sun is equivalent to the nominal solar constant at Earth. Also, Mercury rotates once every 59 days, causing the planet surface temperature to reach steady temperature conditions. Because Mercury's surface absorbs between 90% and 94% of the incident solar radiation, the planet reradiates the equivalent absorbed solar energy in the IR spectrum, creating an extremely harsh IR thermal environment for a spacecraft in orbit or passing close by. The maximum surface temperature at the subsolar point when at Mercury perihelion is  $\sim 430^\circ\text{C}$ ; the temperature decreases  $\sim 300^\circ\text{C}$  at aphelion as the surface temperature distribution and corresponding reradiated heat drop off as a function of the cosine law from the subsolar point to the dawn–dusk terminator. When the spacecraft is in the vicinity of the terminator or is in eclipse over the nightside, the planet's surface temperature is  $-180^\circ\text{C}$ , which is independent of solar distance and drives the thermal environment. The planet surface temperature distribution and corresponding reradiated IR flux distribution as seen by the spacecraft are functions of both solar distance and orbit plane position from the subsolar point. Once in orbit at Mercury, a spacecraft's orbit plane is relatively inertial with respect to the Sun; however, gravitational forces from Mercury and the Sun cause the orbital line of apsides to rotate around Mercury, changing the local position of the orbit periaapsis relative to the subsolar point (Figure 10).

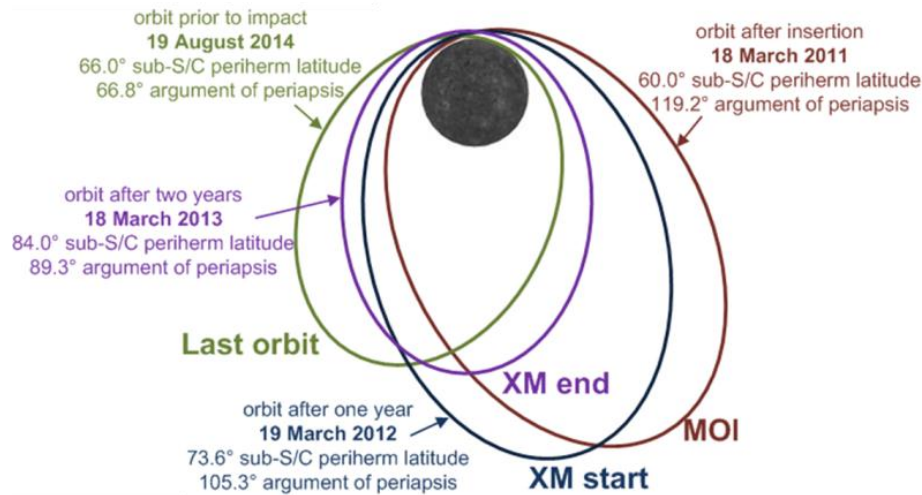


**Figure 10. During the MESSENGER mission, the AP rotates counter-clockwise from an initial position of 119°. The estimated position at the end of the first extended mission (XM) will be 90°. S/C, spacecraft. Figure courtesy of James V. McAdams, APL.**

For MESSENGER, the initial orbit to start the primary mission after the MOI cleanup maneuvers had a nominal orbit geometry of  $200 \text{ km} \times 15,200 \text{ km}$  and an initial inclination and argument of perihelion (AP) of approximately  $82^\circ$  and  $119^\circ$ , respectively. The orbit period was  $\sim 12$  hours (720 minutes), which varied because of perihelion altitude drift. Altitude and orbit period correction burns were alternately performed approximately every 44 days to readjust the perihelion altitude to 200 km and the orbit period to  $\sim 12$  hours.

Because of the highly eccentric spacecraft orbit (eccentricity = 0.74), orbit-averaged heating from the planet can be very misleading. Thermal analysis shows almost no difference in predicted orbit-averaged temperatures for given spacecraft surfaces at very different solar distances when being heated by the planet. This similarity is because the orbital heating from Mercury is integrated and averaged over the 12-hour orbit period. The time that the spacecraft views the planet, during which the orbit altitude range has an effect on the thermal response of a viewing surface, is less than 40 minutes per orbit. When integrated and averaged, the planet thermal effect is almost negligible. Therefore, transient analysis must be used to characterize the thermal response of the spacecraft and identify potential thermal design requirements. During most of the orbit, the spacecraft does not receive much direct heating from Mercury. Consequently, there is a very large thermal recovery period associated with this orbit, which allows the spacecraft to return to a benign initial state before being reheated during the next closest approach. For the MESSENGER mission, the spacecraft was injected into a highly inclined terminator (dawn–dusk) orbit when Mercury was near perihelion, keeping the subsolar crossing (noon–midnight) orbits near MTA  $100^\circ$  and  $280^\circ$ , respectively (Figure 11 and Table 2). Unlike an orbit at Earth, the line of nodes does not regress naturally about Mercury. Orbit plane variations relative to the Sun, measured as beta angle ( $\beta$ ), occur as Mercury moves about the Sun, causing the beta angle to vary proportionally to  $\beta$ , the angular movement of Mercury. Beta angle is defined as the angle between the orbit plane and the sunward direction. When  $\beta$  is zero, the spacecraft travels directly between the Sun and the planet during one point in the orbit, and during that orbit, the spacecraft experiences a seasonal maximum eclipse. During one Mercury year, the beta angle will make one full cycle.

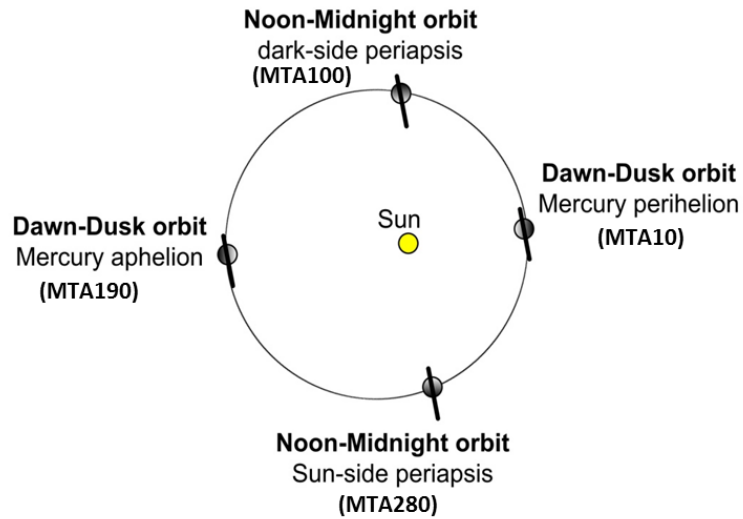


**Figure 11.** Unlike a spacecraft in Earth orbit, the MESSENGER orbit plane is inertially fixed and does not rotate about Mercury’s equator. The orbit plane position relative to the Sun will vary only as a function of MTA.

**Table 2.** The relationship between MTA, solar distance, and MESSENGER orbit plane beta angle

MTA (°)	Solar Distance (AU)	Beta Angle ( $\beta$ )
0	0.300	78.0
10	0.309	83.3
20	0.311	78.0
30	0.316	68.9
40	0.323	59.3
50	0.327	49.5
60	0.337	39.7
70	0.347	29.8
80	0.358	19.9
90	0.370	9.9
100	0.387	0.0
110	0.398	-9.9
120	0.414	-19.9
130	0.428	-29.8
140	0.440	-39.7
150	0.453	-49.5
160	0.460	-59.3
170	0.466	-68.9
180	0.467	-78.0
190	0.464	-83.3
200	0.460	-78.0
210	0.450	-68.9
220	0.439	-59.3
230	0.427	-49.5

MTA (°)	Solar Distance (AU)	Beta Angle (β)
240	0.413	-39.7
250	0.397	-29.8
260	0.386	-19.9
270	0.368	-9.9
280	0.357	0.0
290	0.345	9.9
300	0.335	19.9
310	0.326	29.8
320	0.322	39.7
330	0.315	49.5
340	0.312	59.3
350	0.310	68.9
360	0.300	78.0

## MOI

During the inner cruise phase, the MESSENGER spacecraft approached the Sun at Mercury perihelion distance a dozen times before orbit insertion. These numerous encounters illustrated that the spacecraft thermal design was stable and that critical temperatures were maintained within design specifications and were repeatable (Figure 12). On March 18, 2011, at 00:45 UTC, MESSENGER's 667-N Large Velocity Adjust (LVA) thruster fired for ~15 minutes, slowing the spacecraft by 1,929 miles per hour (862 meters per second) and easing it into the planned orbit about Mercury. During the burn period, the sunshade and deck mounted components on the -Z face of the spacecraft experienced combined thermal environments from solar conditions, which were near maximum, and from LVA operation. As illustrated by Figure 13, the substantial thermal output from the engine was successfully managed by containing the bulk of the radiated thermal energy with Nextel (sunshade-equivalent) blankets, greatly attenuating the direct thermal coupling with critical components such as the battery and solid-state power amplifiers. Components such as the front low-gain antenna and the top DSS head were designed to withstand the Mercury environment, so plume and radiation impingement during the LVA firing did not cause any issues with temperature.

## AN 8- VERSUS 12-HOUR ORBIT PERIOD

From the earliest development of a mission concept for a Mercury orbiter to the implementation of the mission, the MESSENGER spacecraft was designed for a nominal 12-hour orbital period. As explained earlier, the thermal time constant of the spacecraft is such that the passively controlled Mercury viewing components need a high effective thermal mass to prevent overheating during the worst-case transient spike. Consequently, the time to cool to the orbit minimum temperature is proportional to the energy input, the altitude, and the nominal view back to the sunlit side of the planet. During the primary mission, the 12-hour orbit period proved to be adequate during the thermal recovery segment of the orbit. Low effective mass components (e.g., the solar arrays) thermally recovered within an hour after exiting the maximum heating segment of the orbit. The spacecraft adapter, located in the +Z direction and encircling the Mercury direct viewing instruments, has a very high effective thermal mass and came within a few degrees of the achievable orbit minimum.

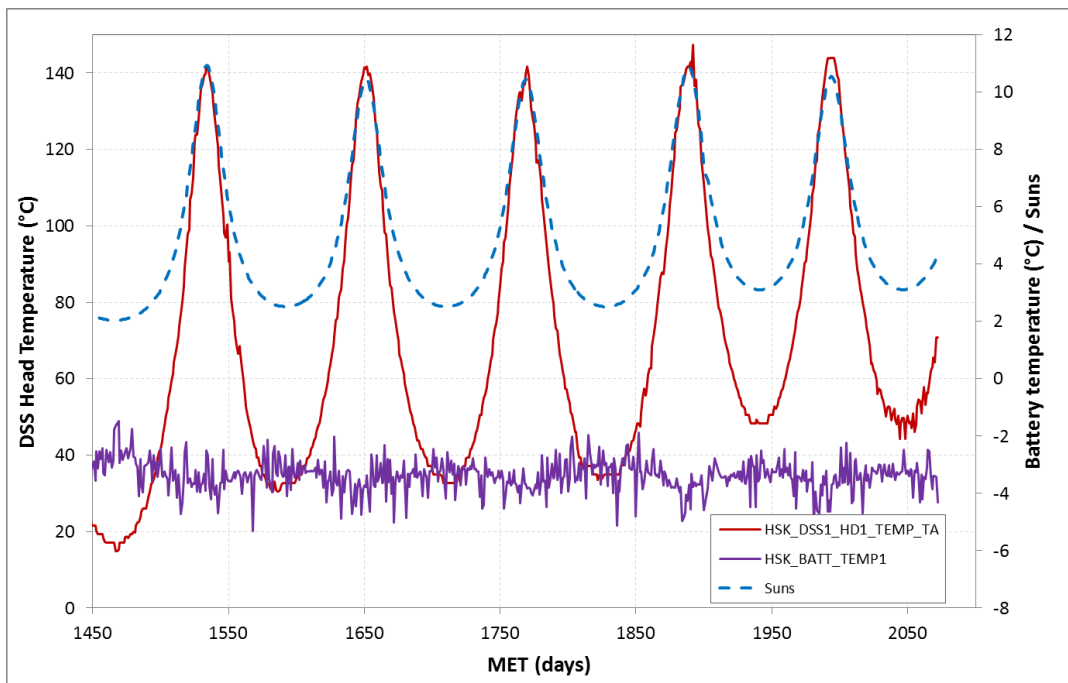


**Figure 12.** Shown here is flight temperature data of one of the four forward-facing DSSs and at the battery. The temperature data are repeatable as a function of solar distance (Suns), indicating that material properties are stable and not degrading. MET, mission elapsed time.

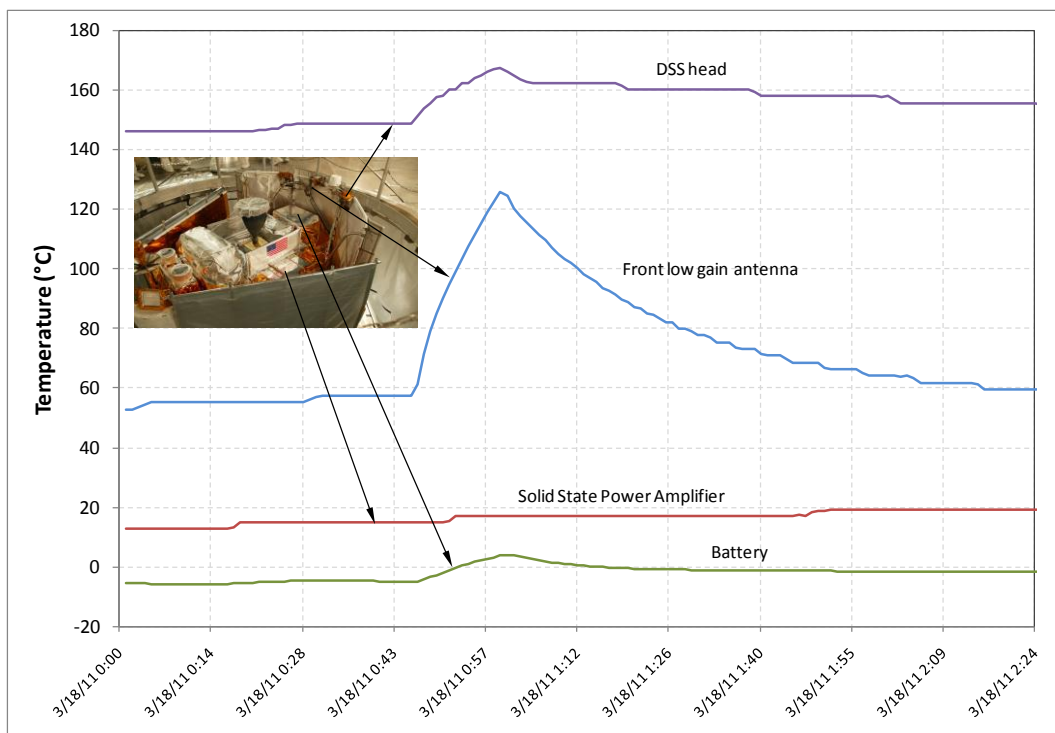


**Figure 13.** Shown is temperature data taken during the 15-minute MOI maneuver. Key components such as the solid-state amplifiers and battery were barely affected, whereas the sunshade-mounted low-gain antenna and upper DSS head saw measurable temperature rises.

When options were being considered for an extension to the primary mission, one proposal was to reduce the orbit period from 12 to 8 hours (480 minutes) by keeping periapsis at ~200 km and reducing apoapsis from 15,200 km to ~10,000 km. The major benefit in going to the 8-hour orbit is that the spacecraft experiences three orbits per day instead of two as well as greater integrated time at lower altitude. The initial concern in moving to the shorter orbit period was that the spacecraft would be adversely affected by the shorter orbit period and the potential of higher background thermal radiation from Mercury due to the smaller effective orbit diameter. Comprehensive system-level thermal analysis was performed to simulate the differences in the two orbit geometries as well as time constant effects on spacecraft components. During the most intense heating segment of each orbit, which occurs at the lowest altitudes, per Figure 14, the 8- and 12-hour orbits are nearly identical, with the maximum calculated difference being less than 10% higher for the 8-hour orbit. During the recovery segment of the orbit when elapsed time and spacecraft distance from Mercury factor into the temperature performance, thermal analysis modeling both orbit scenarios as well as variation in AP were done. For the orbits being analyzed, the drift in AP is the about the same and has to be factored into the analysis. Once again, looking at a component that represents a low effective thermal mass, the solar arrays were analyzed for both the 8- and 12-hour orbits. As illustrated by Figure 15, predictions show the solar-array performance to be nearly identical for both orbit geometries when using the same angles for operation and safe tilt. However, for a high effective thermal mass component such as the adapter, per Figure 16, the difference in peak temperature increases ~10°C for the 8-hour orbit compared with the 12-hour orbit. For the passively controlled adapter, Figures 14 and 16 also illustrates the effect of AP shift on expected spacecraft heating and temperature. As shown, the Out-Bound Season (OBS) and In-Bound Season (IBS) parts of the Mercury orbit effectively “switch” relative to peak temperature profiles. The OBS is defined as going from Mercury perihelion to Mercury aphelion (MTA 0° to 180°), and the IBS is defined as going from Mercury aphelion to Mercury perihelion (MTA 180° to 0°). Because of gravitational effects, the orbit AP rotates from 120° initially to 90° by the end of the extended mission. Because of the changing orbit geometry, as the AP reduces over time, the peak temperature of the adapter will increase during the OBS and decrease during the IBS.

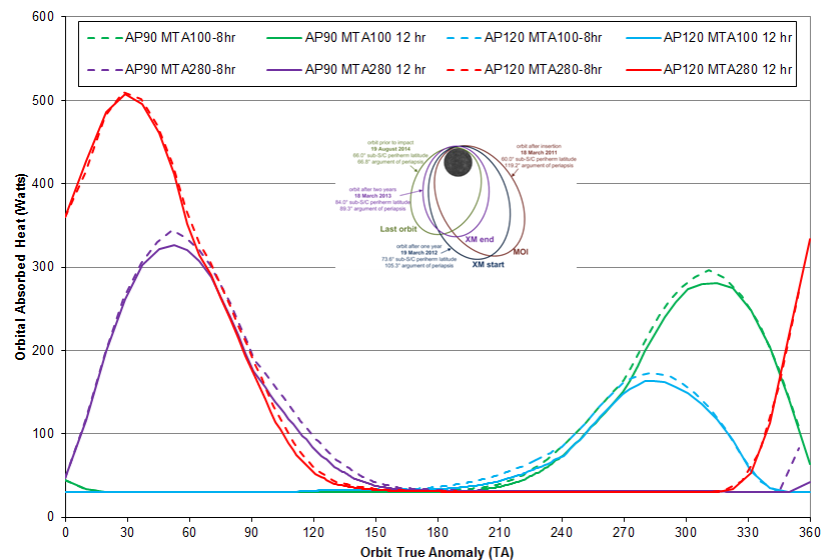


**Figure 14.** During the maximum heating segment of each orbit, the 8- and 12-hour orbits are nearly identical and independent of argument of periapsis (AP). TA, true anomaly.

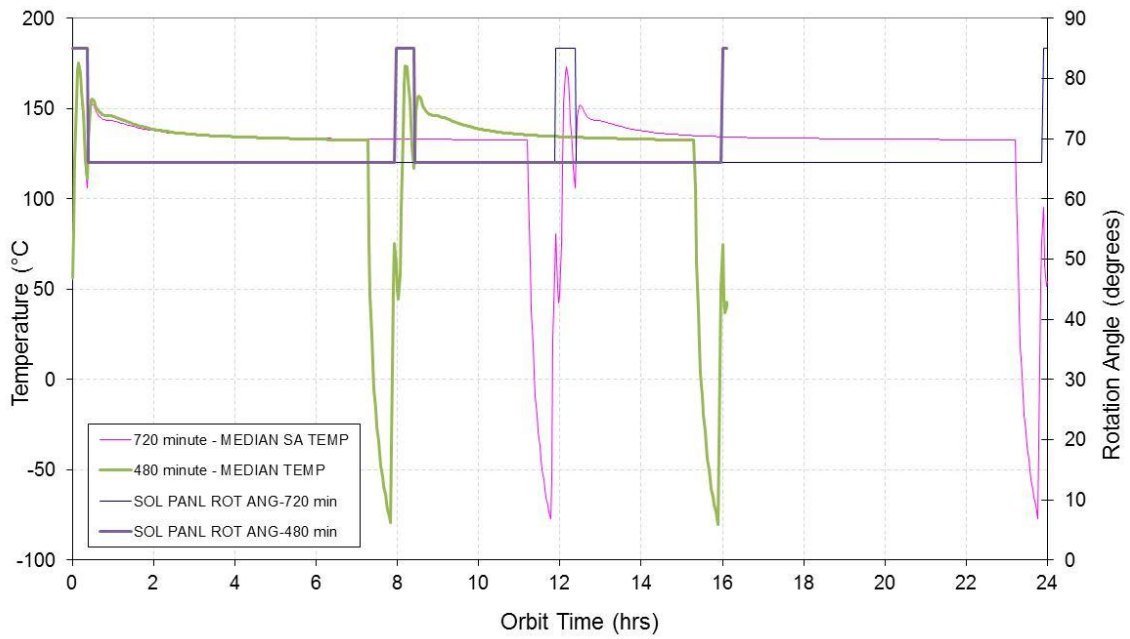


Figure 15. As shown here, solar-array thermal performance is nearly identical for 8- and 12-hour geometries for given angles for operation and safe tilt.

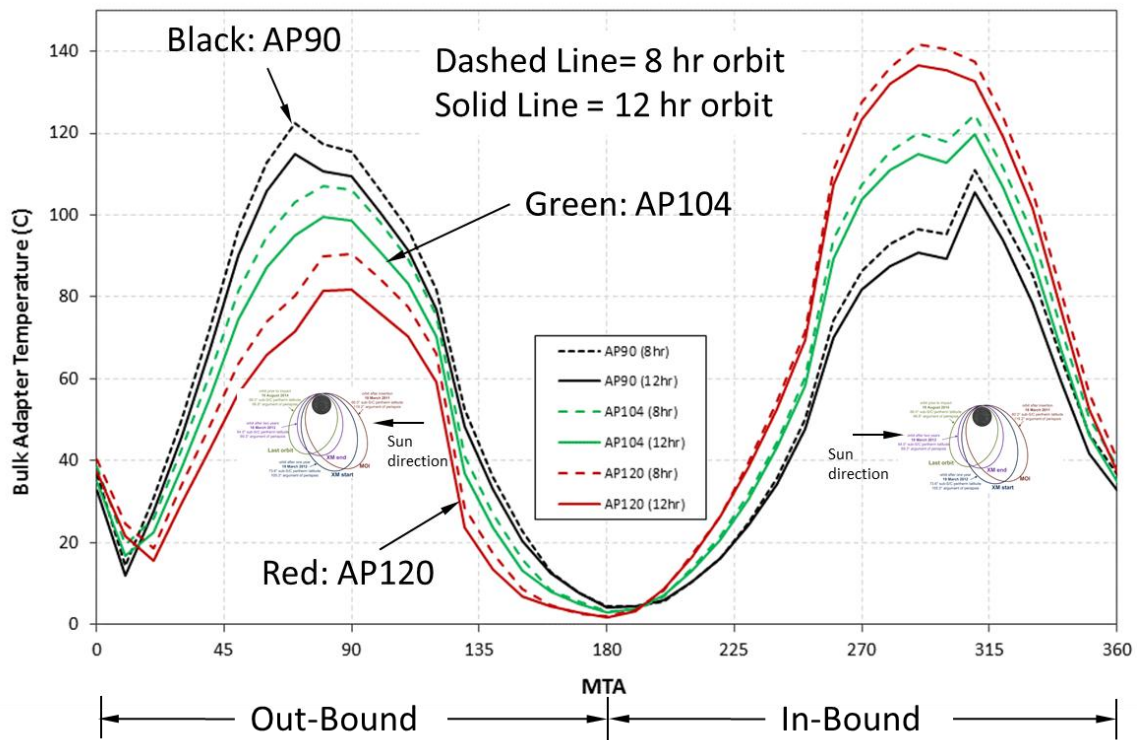
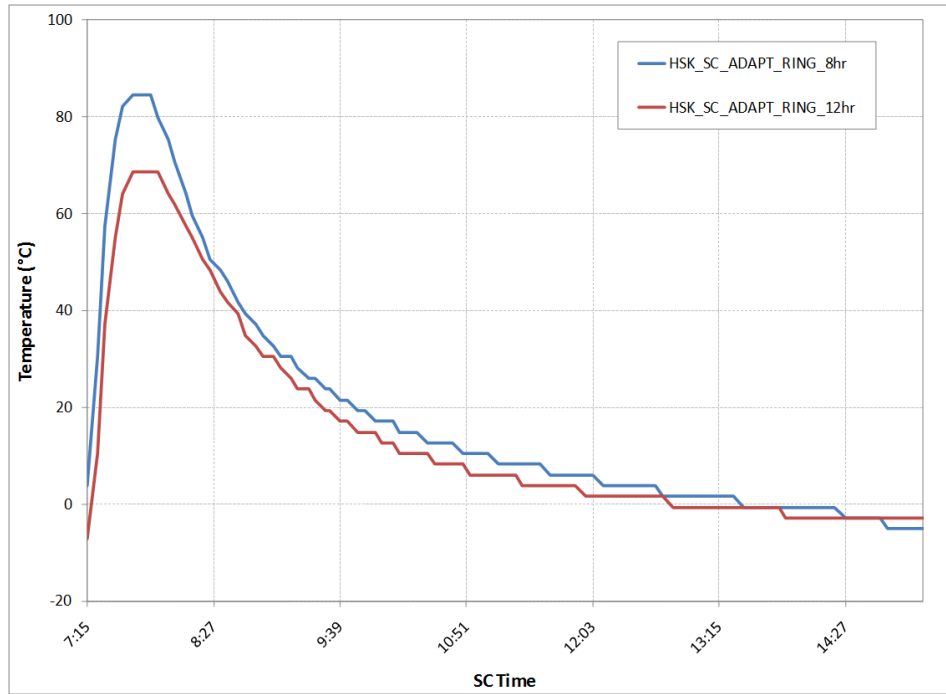
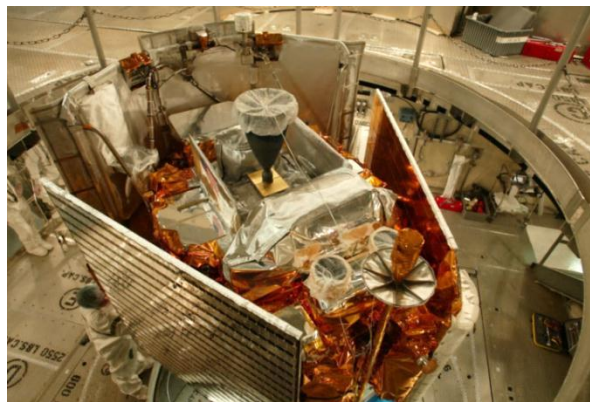


Figure 16. As the orbit AP rotates northward, the seasonal temperature profiles change as well. As shown, the OBS and IBS parts of the Mercury year effectively “switch” relative to peak temperature profiles during the lifetime of the mission.

Because the spacecraft had already completed the primary mission and analytical simulations comparing the effects of 8- and 12-hour orbit periods showed an  $\sim 10^{\circ}\text{C}$  difference in the peak temperature during the highest heating portions of each OBS and IBS, it was decided to pursue the 8-hour orbit geometry for the extended mission. On April 20, 2012, the MESSENGER spacecraft completed the second of two maneuvers that reduced the orbital period from 12 hours to 8 hours. The final orbit correction burn occurred at MTA  $195^{\circ}$ , near the start of the IBS for Mercury year 5. The flight data depicted in Figure 17 show the  $10^{\circ}\text{C}$  peak difference in adapter temperature for 8- and 12-hour orbits at MTA  $267^{\circ}$  environmental conditions. Spacecraft and instrument performance is discussed further below.



**Figure 17.** The flight data depicted in this figure verify the  $10^{\circ}\text{C}$  peak difference in adapter temperature that was predicted between 8- and 12-hour orbits at MTA  $267^{\circ}$  environmental conditions.



**Figure 18.** Shown is a view of the spacecraft before launch, with solar arrays in stowed positions. It is hypothesized that excessive IR trapping between the spacecraft and sunshade is contributing to the RF connector temperature increase.



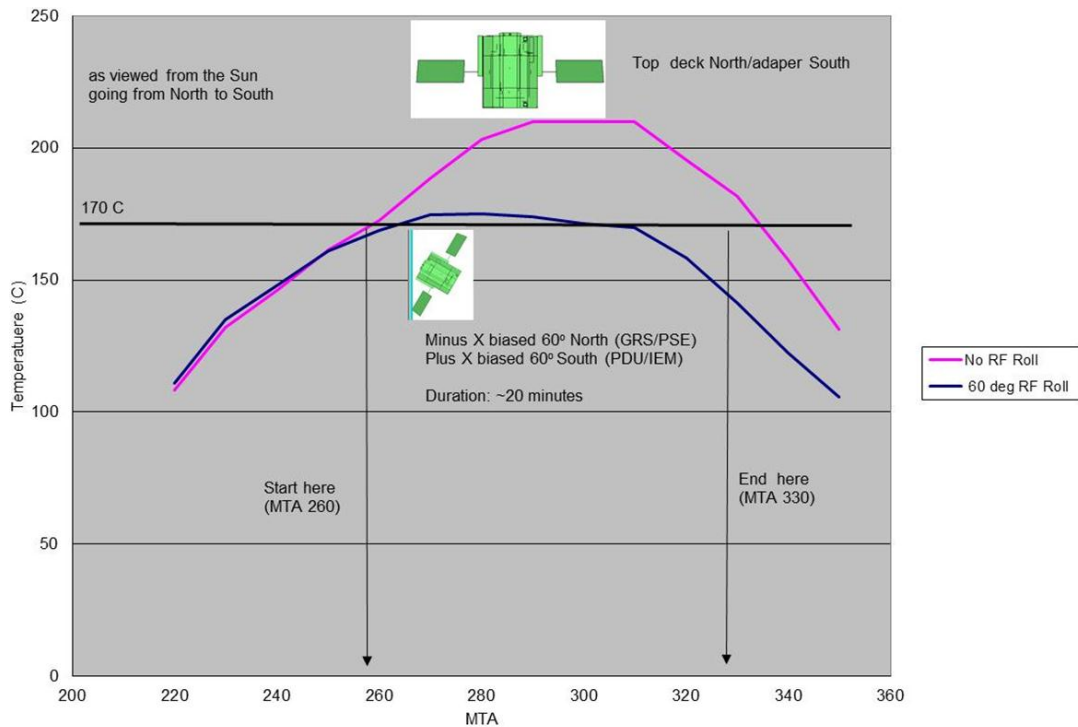


**Figure 19. The thermal effects of a spacecraft roll around the Y axis (Sun line) were analyzed and compared to the results of the nominal spacecraft attitude. Per the analysis, it was shown that by biasing +X toward the planet, the -X and +Z thermal environments as seen by the antenna would be sufficiently reduced to protect the antenna from thermal damage.**

### FRONT PHASED-ARRAY ANTENNA THERMAL MITIGATION

From flight data analyzed during the first 30 days of the mission, it was estimated that the signal feeds for front phased-array and fan-beam antenna assembly could exceed qualification temperatures at the highest thermal input, which would occur during the inbound portion of the first hot season. As previously illustrated, the peak heating, especially on external spacecraft components, was predicted to occur during the IBS when the spacecraft is near MTA 310°. No electronics are affected, but the antenna feed assembly is soldered with SN63, which has a melting temperature of ~180°C. As shown in Figure 18, the antenna is located around the midpoint on the -X side of the sunshade. It is hypothesized that excessive IR caused by heat flux along the -X and lesser +Z directions is being trapped between the spacecraft and sunshade and is contributing to the radio frequency (RF) connector temperature increase. If signal continuity to part of the phased-array antenna is lost, then antenna output during downlink would be lower in proportion to the number of sticks that were compromised (1 stick = 1/8 gain to system or ~12.5% lower gain if damaged) [7]. If signal continuity is lost or degraded to the front fan-beam antenna, the spacecraft would lose the ability to receive high-gain uplink for the part of the mission when the spacecraft-to-Earth orbit geometry dictates the use of the front antenna assembly. A mitigation plan that was devised to protect the antenna from the expected high thermal flux while minimizing the effect on spacecraft normal operations was quickly studied and implemented. Because the phased array was not transmitting and the attitude-dependent instruments were not obtaining data during hottest points of the IBS orbits, the plan to protect the antenna was to reduce the -X and +Z view to the planet during a window around periapsis passage. Thermal analysis correlated to the first OBS antenna temperature data and spacecraft attitude predicted that during the peak heat portion of the first IBS, the antenna could have easily

exceeded 200°C and possibly sustained damage. A 60° spacecraft roll around the *Y* axis (Sun line) was analyzed (Figure 19) to determine whether such a maneuver would benefit the antenna situation and, if so, where in the orbit and over what range of MTA it would have to be implemented. Per the analysis, it was shown that by biasing +*X* toward the planet, the −*X* and +*Z* thermal environments as seen by the antenna were sufficiently reduced to protect the antenna from thermal damage. So starting on May 24, 2012 (MTA 250°), attitude alterations began and continued through June 8, 2012 (MTA 320°). Starting on June 3, 2012, the guidance, navigation, and control (GNC) team implemented two separate off-pointing algorithms to handle high slew rates and top-deck constraints as well as limited off-pointing, in order to reduce science impact. The RF off-pointing lasted for ~25 minutes during each orbit, successfully attenuating the high heat from Mercury on the antenna while pointing the +*X* side of the spacecraft to a near nadir attitude, causing the +*X* diode heat pipe radiator panels to activate. The flight data shown in Figure 20 illustrate how effectively the thermal control design “shuts down,” keeping Mercury’s intense heat away from critical electronics such as the SAJB while ensuring that the phased-array antenna critical temperature stays well below 180°C. The RF off-point will continue for the remainder of the mission; however, because of the rotation of AP, the MTA range and orbital duration will be reduced accordingly in order to take advantage of the lower seasonal heating.

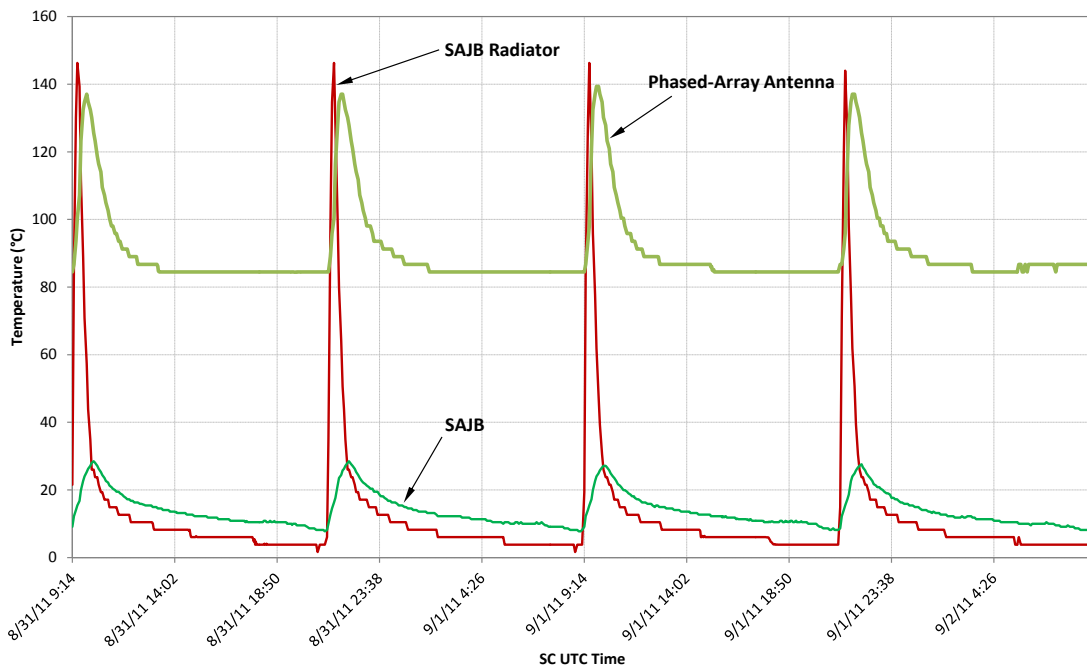


**Figure 20. The flight data shown here illustrate how effectively the thermal control design “shuts down,” keeping Mercury’s intense heat away from critical electronics, such as the SAJB, while keeping the phased-array antenna critical temperature well below 180°C.**

## SOLAR-ARRAY OPERATION

The baseline plan for solar array temperature control has always been to strategically off-point each wing during the highest peak heating part of orbits that range from MTA 220° to 350° while keeping the peak median temperature of each wing at less than 180°C. During the first Mercury year, when the orbit AP was initially ~119°, the MTA 280° orbit represented not only a near maximum thermal condition but also the most power-constrained orbit of the mission because of the 62-minute maximum eclipse. During this family of orbits, instrument operations were constrained because of concerns over battery depth of discharge when the arrays were in a non-

power-producing orientation. Per the MTA 280°/AP 119° solar-array simulation shown in Figure 21, the solar arrays experience a 62-minute eclipse, during which the minimum temperature reached is -110°C; this eclipse is followed by ~20 minutes of high-solar-intensity heating, during which the battery is partially recharged, followed by the subsolar point crossing, near which orbit periapsis is at ~60° north latitude and the solar arrays are edge-on to the Sun for ~25 minutes and not generating power. As part of the ongoing power and thermal solar-array management, thermal analysis is performed per Mercury year to account for orbit geometry differences induced by the rotation on the line of apsides. Figure 22 is a comparison of the analysis done at the beginning of the mission, when the initial AP was 119° and the orbit period was 12 hours, to what is expected at the end of the first extended mission, when the AP is calculated to be 90° and the orbit period will be 8 hours. At the beginning of the mission, no active solar-array control was performed during the OBS, but as illustrated, in order to keep array temperatures in the desired range, the wings will need to be off-pointed for ~30 minutes per orbit, from about MTA 30° to about MTA 140°. Note that the maximum eclipse for the OBS and IBS is still at MTA 100° and 280°, respectively; but the maximum eclipse times have increased by ~10 minutes during the OBS and decreased by ~22 minutes during the IBS as the AP increases from 119° to 90°.

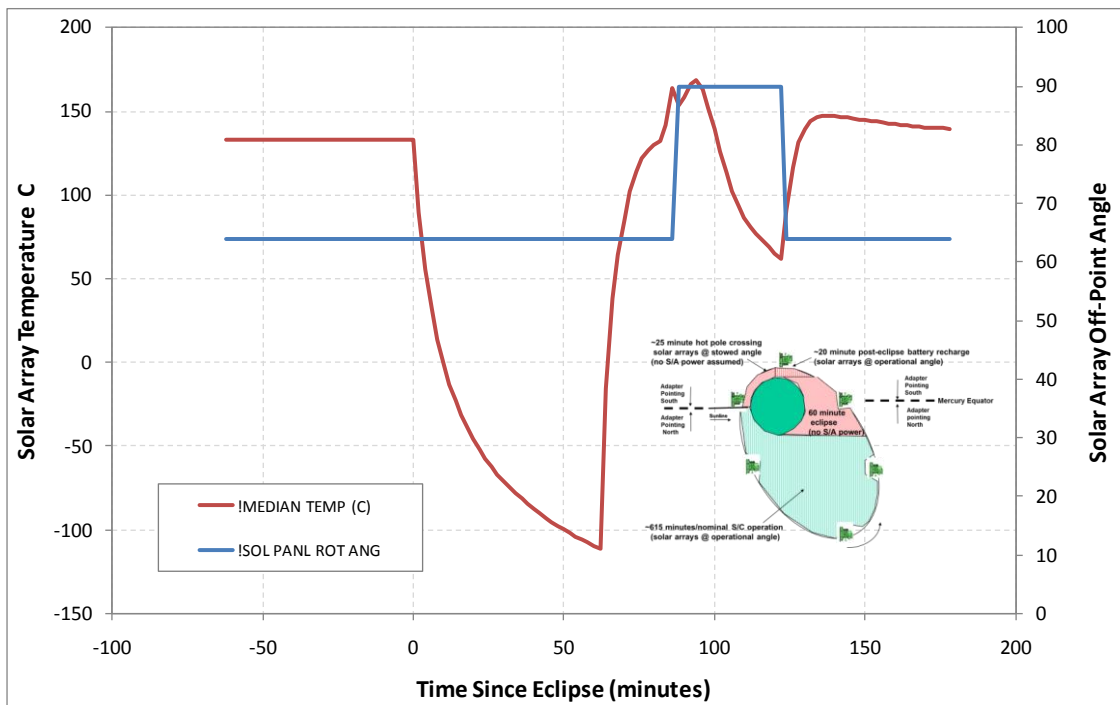


**Figure 21. During solar-array management, the objective is to keep the median peak array temperature at less than 180°C during the hottest part of the orbit. Per the solar-array simulation shown, the solar arrays must be maintained edge-on to the Sun for ~25 minutes and, as a consequence, does not generate power.**

## SPACECRAFT OPERATION AND PERFORMANCE SUMMARY

The thermal control system for the MESSENGER spacecraft has performed well during the orbital phase of the mission. Since MOI, spacecraft temperatures and other housekeeping telemetry have been processed and catalogued per orbit, and minimum, maximum, and orbit-average temperatures have been published as a function of MTA for each Mercury year. This summary information for the adapter, current to Mercury year 6 MTA 161° as of the time of this writing, is

shown in Figure 23. The OBSs and IBSs, mentioned previously, can clearly be seen in the figure. The temperatures at the peak of the OBS are seen to drift upward for each Mercury year, caused by the drift in the orbit AP. The corresponding decrease in temperatures at the peak of the IBS for each Mercury year is masked by attitude and operational constraints placed on the spacecraft during this season, as well as the change to an 8-hour orbit around MTA 190° in Mercury year 5. When plotting the temperature extremes per orbit as a function of MTA, the temperature response of any given spacecraft component is seen against the backdrop of data from the previous Mercury year, which is very useful in understanding the thermal state of the spacecraft.

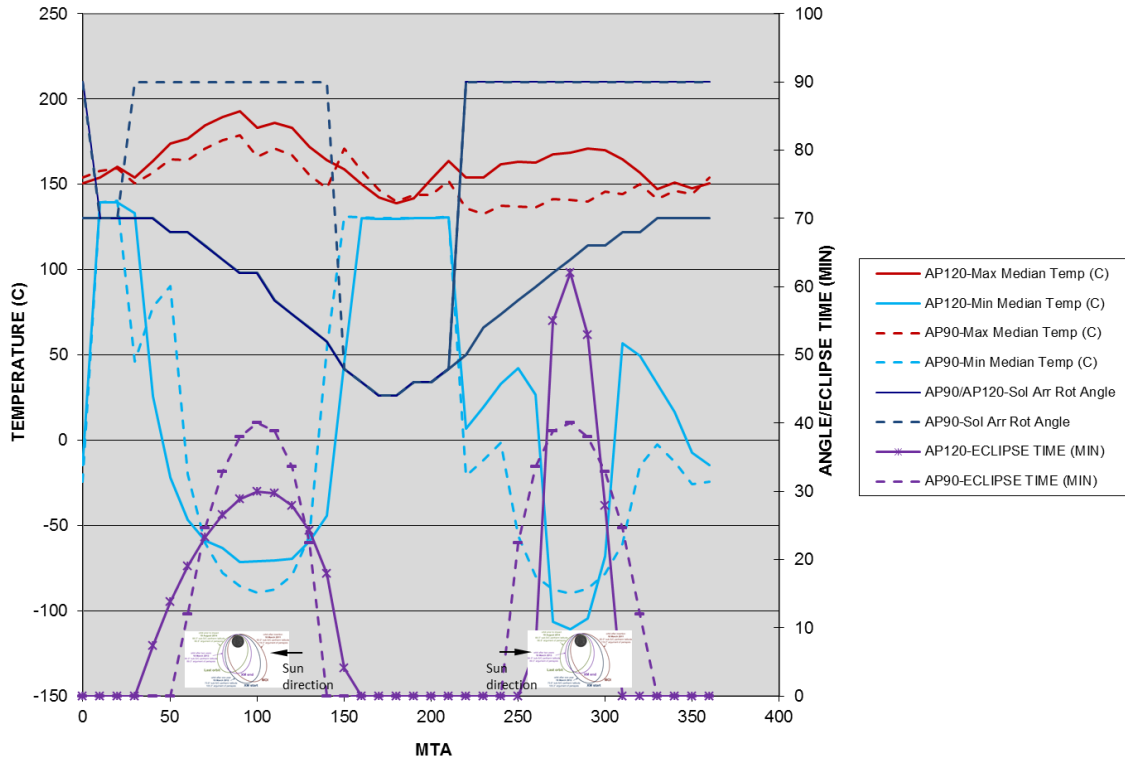


**Figure 22. A comparison of the analysis done at the beginning of the mission, when the initial AP was 119° and the orbit period was 12 hours, to what is expected at the end of the first extended mission, when the AP is calculated to be 90° and the orbit period will be 8 hours. Note that the maximum eclipse for the OBS and IBS is still at MTA 100° and 280°, respectively; however, the maximum eclipse times have increased by ~10 minutes during the OBS and decreased by ~22 minutes during the IBS as the AP increases from 119° to 90°.**

The orbital temperature response of most spacecraft hardware is seen to be a strong function of the spacecraft position and attitude in orbit, in addition to the season. In Figure 23, the adapter temperature generally follows a smooth transition in and out of the OBSs and IBSs, with step changes in temperatures at certain MTA values. For example, the temperatures drop steeply at MTA 270° because of the imposed spacecraft off-pointing rules, mentioned previously. Early in the orbital phase of the mission, specific scenarios were analyzed with the actual spacecraft attitude profile through the use of the external spacecraft model in commercial thermal software in order to better understand situations that occurred. Later in the mission, heat rates for all orbits were run for the predicted spacecraft attitude profile and characterized in a similar fashion as the temperature telemetry. To limit the large amount of data and processing time that these calculations would entail, the bulk heat-rate processing was limited to the environmental heating

on the principal spacecraft directions (six faces of a cube). A code was written for this purpose to integrate the IR heating from the planet surface, which varies in temperature according to the solar direction vector, on the faces of a cube with the correct spacecraft position and attitude as a function of time. The code also factors in the solar distance for the heating calculation, determines the MTA value for each time step, contains a trigger to limit orbit steps yet include any for which the position or attitude changes more than a given amount, and segregates the data on the basis of orbit periapsis passage times to seamlessly fold the heat-rate data into the existing temperature telemetry process. The heat rates for the +X direction are shown in the upper portion of Figure 24, whereas the SAJB radiator temperatures are shown in the lower portion. A strong correlation between the heat rates and temperatures is seen in the chart, a result that is expected because the radiator is on the +X side of the spacecraft. Similar correlations are seen with other spacecraft hardware, especially radiators. Note that heat-rate calculations extend beyond the current time because they are calculated from the planned spacecraft attitude. This forecasting allows the near-term plan for science and guidance and control for the spacecraft, as it is being generated, to be directly evaluated for thermal concerns and modified accordingly. The small black triangle in the figure indicates the time before which final spacecraft attitudes have been processed, whereas the yellow triangle indicates the time beyond which only long-term spacecraft attitude predictions have been processed.

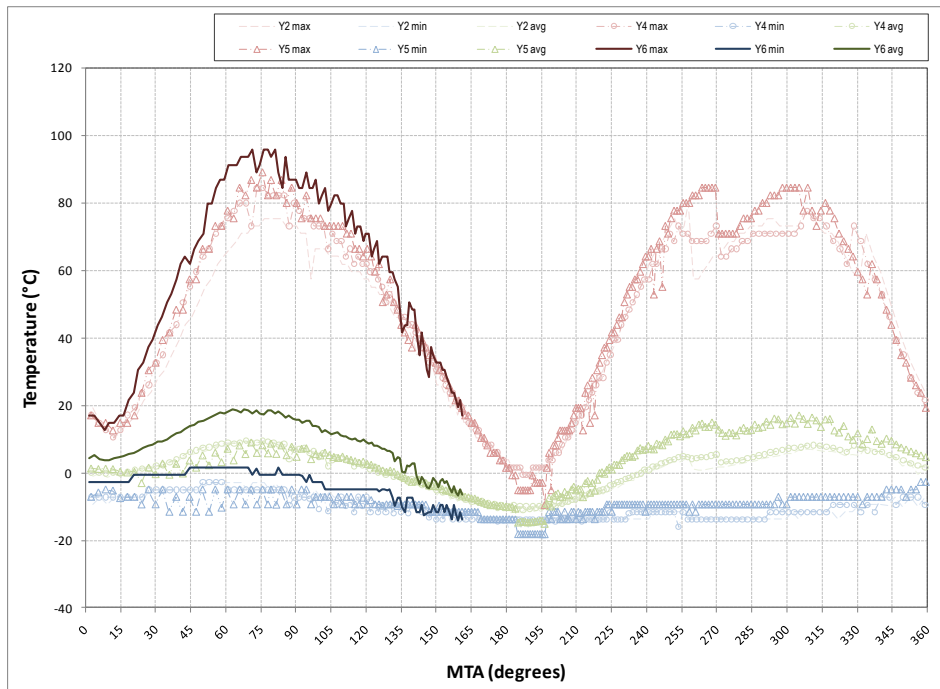


**Figure 23. The OBSs and IBSs, described in the text, can clearly be seen. The temperatures at the peak of the OBS are seen to drift upward for each Mercury year, caused by the drift in the orbit AP. The sharp temperature step change around MTA 270° is due to the spacecraft attitude adjustment for RF off-pointing.**

Using the post-processing techniques described here, it is apparent that the spacecraft thermal performance is repeatable, predictable, and well understood. Furthermore, now that heat-rate predictions are folded into the planning process, thermal constraints are resolved in greater detail and early enough to allow for even more science measurements to be obtained.

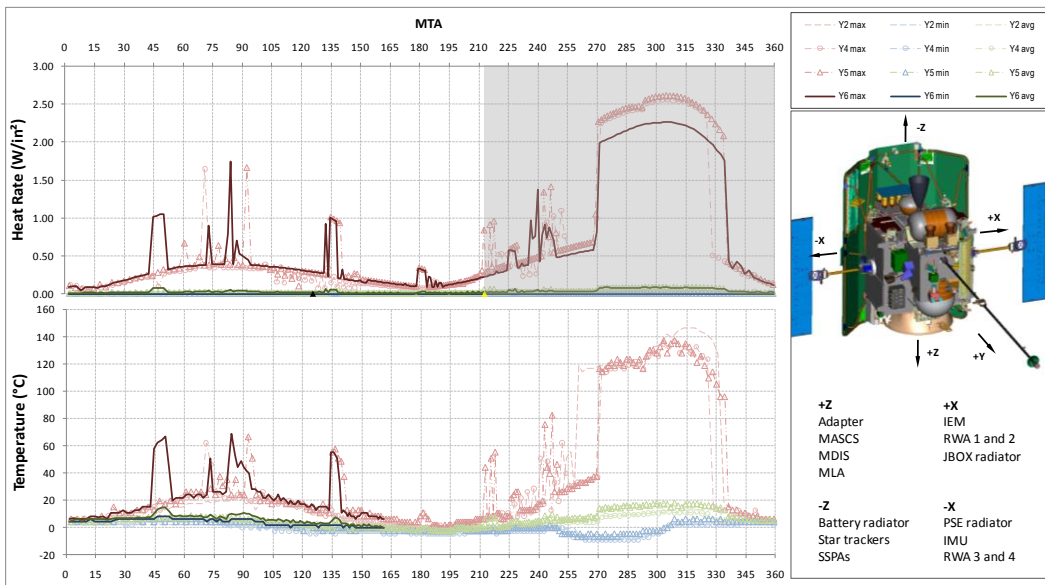


**Figure 24. Comparison of the calculated heat rates for the spacecraft +X direction (upper panel) with the SAJB radiator temperatures (lower panel). A strong correlation between the heat rates and temperatures is seen in the chart, which is expected because the radiator is on the +X side of the spacecraft. JBOX, Junction Box; RWA, Reaction Wheel Assembly; SSPA, Solid-State Power Amplifier.**

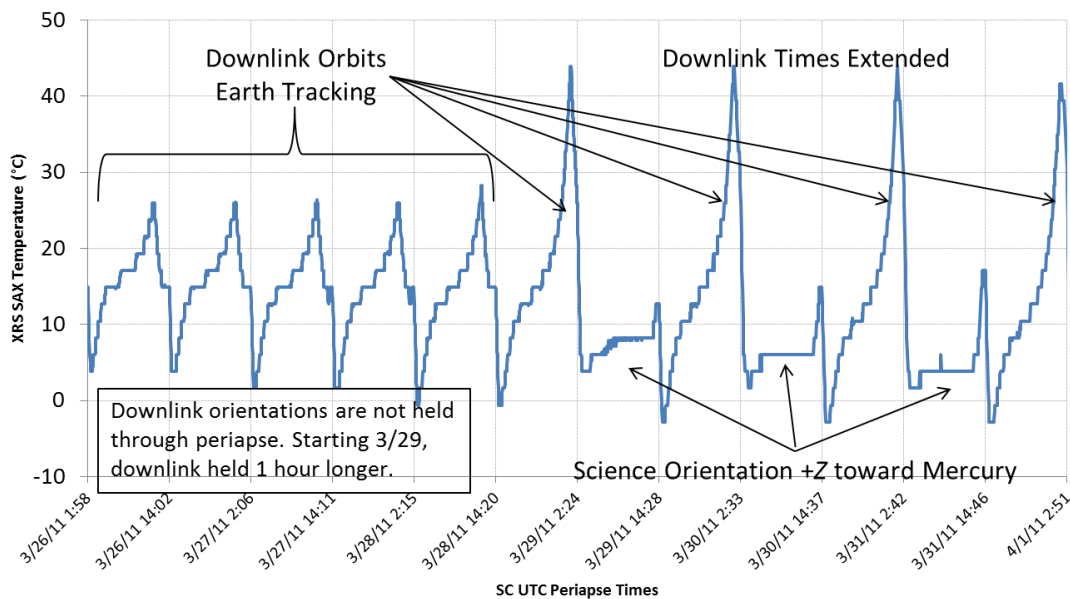


**Figure 25. Shown are the effects of downlink attitudes and timing on the XRS SAX. The observed dependence on spacecraft attitude by this and other instruments highlighted the importance of monitoring planned spacecraft maneuvers and limiting exposure of sensitive surfaces to the planetary dayside surface.**

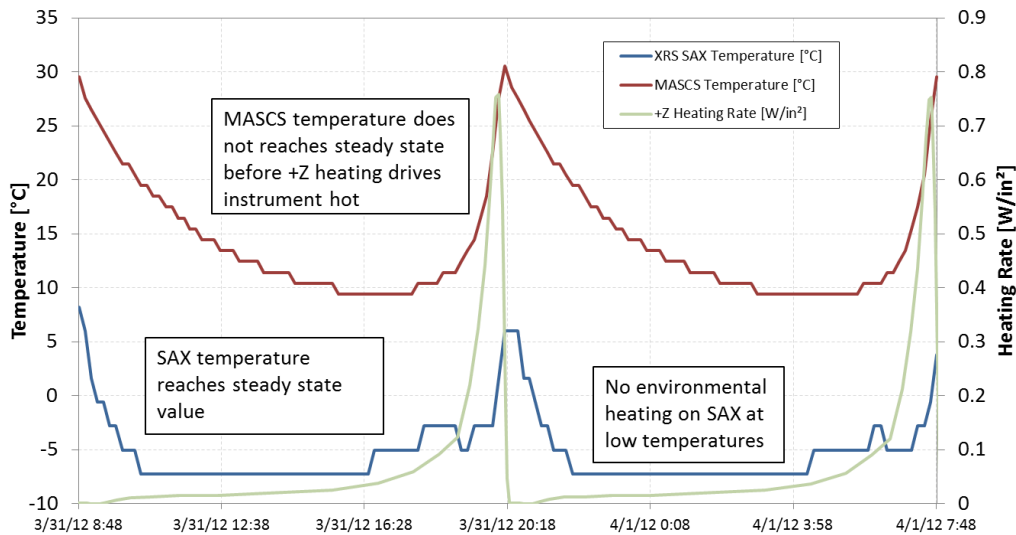


**Figure 26. Shown here is the typical orbital response to high heating rates for the sunshade-mounted SAX and the adapter-mounted MASCS instruments.**

## INSTRUMENT OPERATION AND PERFORMANCE

MESSENGER's instruments experience an extreme range of environments, have a wide variety of scientific goals, and utilize many unique design concepts to achieve their objectives. The extremes of the actual Mercury orbit test some instrument designs more than expected in the design phase, pushing instrument temperatures above the expected operational range. Since the highest solar fluxes were first experienced near the time of the first Mercury flyby, the departures from thermal design predictions have been examined, and assumptions have been modified to allow improved predictions. Further improvements have been incorporated to address issues arising after MOI.

Spacecraft attitude was quickly recognized as a major control on thermal state for some instruments. Idealized orbits in the design phase kept the +Z axis of the spacecraft rotated around the Sun line toward the center of the planet as a default orientation. This orientation is commonly used in practice because it allows the directional instruments inside of the adapter ring to take measurements of their target, but necessary operations such as limb scans, calibrations, off-nadir pointing, and downlink attitudes result in variations to the thermal environments. Figure 25 shows the effect of downlink attitudes and timing on the X-Ray Spectrometer (XRS) Solar Assembly for X-rays (SAX). The observed dependence on spacecraft attitude by this and other instruments highlighted the importance of monitoring planned spacecraft maneuvers and limiting planetary exposure of sensitive surfaces. Because off-nadir pointing is unavoidable, examination of the expected heating rates in each command load has become an important strategy in avoiding unexpected temperature peaks while enabling necessary maneuvers.

In general, most instrument temperatures have shown patterns similar to those seen for the spacecraft during the first four Mercury years with its 12-hour orbit. A typical orbital response to high heating rates has been a sharp increase followed by an approximately exponential decay in temperature toward a steady-state level that may never be reached because of either the long instrument thermal time constant or the response of a heater (Figure 26). In small light instruments (e.g., SAX), the decay is rapid, with equilibrium temperatures obtained within a short period of time (~3 hours after the peak heating event). For these instruments, no change in peak temperature

is expected from the change to an 8-hour orbit. Their time constants are sufficiently short that they retain no memory of the previous heat flux peak when the next heat pulse arrives. Other instruments react more slowly, with temperatures continuously cooling until the next heating pulse causes another jump in temperature reflecting the environmental load received.

Many of the instruments have powered off to avoid the periods of highest heat flux during the inbound hot season. The resulting decrease in internal dissipation reduces instrument temperatures and allows passage through the extremes. Power system limitations have driven some of this instrument inactivity, but some of these limitations are being removed as the AP and IBS heat fluxes are reduced, as shown in Figure 16. With the power system limitations reduced, thermal limits will require power cycling of the Mercury Atmospheric and Surface Composition Spectrometer (MASCS) to maintain safe temperatures. Additional modeling and temperature prediction work will continue in order to maximize science returns within the thermal limits protecting the instrument. The Mercury Laser Altimeter (MLA) successfully completed the primary mission but has gradually experienced laser degradation from firing at temperatures  $>30^{\circ}\text{C}$ . A new autonomy rule was added to prevent laser activity at greater than  $30^{\circ}\text{C}$  and prolong instrument life. The combination of the new limit, increasing OBS heating rates, and the 8-hour orbit would have resulted in many orbits with no MLA science. A new thermal management scheme has been implemented and refined that bypasses the inflexible instrument thermal control system to cool the instrument bulk below its designed operating temperature so that the heating pulse near periaapsis will not raise the temperature so much that a shot cannot be fired.

## SUMMARY

On March 29, 2011, at 5:20 a.m. EDT, MESSENGER captured the historic image of Mercury shown in Figure 27 with the wide-angle camera (WAC) of the Mercury Dual Imaging System (MDIS). This image is the first ever obtained from a spacecraft in orbit about the Solar System's innermost planet and, to date, MESSENGER has taken in excess of 100,000 images and completed  $>1,000$  orbits.

Overall, the MESSENGER spacecraft thermal control design has performed very well, as supported by the data presented in this paper. A summary of minimum and maximum component temperatures for the orbital phase compared with the flight acceptance limits (Table 3) illustrates well this general assessment.

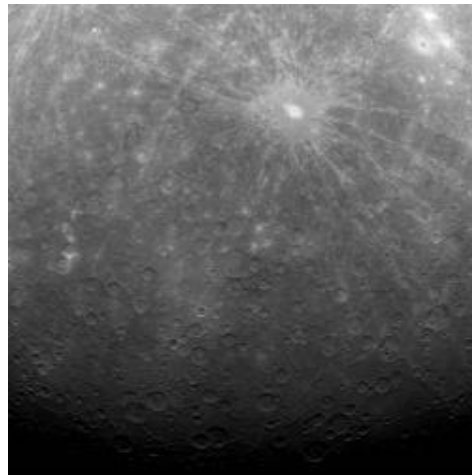


**Figure 27. This image, captured using the MDIS WAC, is the first ever obtained from a spacecraft in orbit about Mercury. To date, MESSENGER has taken in excess of 100,000 images and completed in excess of 1,000 orbits.**



**Table 3. A summary of measured minimum and maximum component temperatures to date**

Component	Mercury year 1		Mercury year 2		Mercury year 3		Mercury year 4		Mercury year 5		Mercury year 6, to date		Mercury years 1-6		Acceptance		Margin	
	min	max	min	max	min	max	min	max	min	max	min	max	min	max	low	high	cold	hot
Adapter	-16	94	-16	80	-16	78	-16	84	-18	89	-14	96	-18	96	-20	100		
SA3 -X	-107	221	-106	214	-100	215	-98	220	-92	199	-74	199	-107	221	-140	230	33	9
SA1 +X	-111	193	-109	186	-103	194	-102	200	-95	178	-78	178	-111	200	-140	230	29	30
ReactionWheels	23	56	23	50	23	49	24	52	23	54	26	54	23	56	-40	70	63	14
FrontLowAntenna	-1	126	2	132	2	128	4	126	8	135	13	89	-1	135	-100	150	99	15
FrontPhaseAntenna	44	167	44	144	46	158	46	158	45	172	51	165	44	172	-100	150	144	-22
VCO	12	47	14	45	12	45	13	46	16	49	17	52	12	52	-34	60	46	8
SSPA	-7	30	-7	35	-12	37	-7	33	-9	37	-7	35	-12	37	-34	50	22	13
StarTracker	-6	19	-6	19	-6	19	-6	18	-6	22	-5	17	-6	22	-34	65	28	43
IMU	-1	33	2	37	2	35	2	35	4	39	6	44	-1	44	-24	65	23	21
DSADhotSide3	73	191	75	184	75	179	75	179	75	181	80	174	73	191	-85	185	158	-6
DSADhotSide1	71	167	71	167	71	165	71	163	73	160	73	153	71	167	-85	185	156	18
Boxes	-7	41	-8	41	-6	40	-6	39	-9	43	-4	43	-9	43	-34	65	25	22
Tanks	13	33	13	30	13	32	14	32	12	36	14	35	12	36	0	50	12	14
HeTank	5	25	7	17	4	22	6	17	6	22	9	21	4	25	0	50	4	25
Battery	-6	7	-5	9	-5	10	-5	9	-5	12	-5	4	-6	12	-10	25	4	13
MDIS	-45	43	-33	45	-31	46	-32	47	-39	47	-29	60	-45	60	-50	50	5	-10
MASCS	-15	48	-3	52	-2	53	-1	55	-18	56	3	65	-18	65	-30	50	12	-15
EPS	-37	22	-34	22	-15	27	-14	22	-39	24	-12	21	-39	27	-30	45	-9	18
FIPS	-3	23	3	22	3	21	4	21	-1	24	7	26	-3	26	-30	65	27	39
MAGbox	5	35	16	33	14	33	15	31	11	32	13	32	5	35	-34	65	39	30
MAGsensor	-128	105	-128	96	-128	91	-120	96	-111	107	-103	132	-128	132	-135	135	7	3
XRSmxu	-17	47	-1	49	0	50	-1	51	-18	49	10	59	-18	59	-30	65	12	6
XRSsax	-29	57	-27	66	-25	62	-25	60	-20	64	-9	46	-29	66	-50	65	21	-1
NUSsens	-21	18	-12	13	-14	13	-13	14	-12	17	-7	19	-21	19	-30	50	9	31
MLAbody	-14	42	-13	44	-13	40	-13	43	-14	40	-13	50	-14	50	-30	50	16	0
PDU	5	32	7	33	5	32	6	32	7	34	10	38	5	38	-34	65	39	27
PSE	-12	22	-11	22	-10	21	-10	24	-8	24	0	32	-12	32	-34	70	22	38
PSERad	-16	53	-16	84	-16	60	-16	57	-12	84	-7	69	-16	84	-50	240	34	156
GRSbox	16	42	16	41	18	40	14	43	9	45	7	51	7	51	-34	65	41	14
GRScomp	-16	49	-16	58	-16	41	-16	44	-15	49	-19	54	-19	58	-45	60	26	2
SAJB	-8	27	-5	28	-5	27	-6	26	-2	29	5	31	-8	31	-30	75	22	44
SAJBrad	-12	135	-9	146	-9	142	-9	137	-7	137	-1	69	-12	146	-50	240	38	94
OEXO	16	37	16	37	16	37	17	36	16	40	19	39	16	40	-25	60	41	20

## ACKNOWLEDGMENTS

The MESSENGER mission is supported by the NASA Discovery Program under contracts to CIW and APL. The author acknowledges Sean Solomon, the MESSENGER spacecraft Principal Investigator at CIW, and Peter Bedini, the MESSENGER spacecraft Project Manager at APL, for their support in the preparation and presentation of this paper.

## REFERENCES

- <sup>1</sup> C. L. Yen, "Ballistic Mercury Orbiter Mission via Venus and Mercury Gravity Assist." *J. Astronaut. Sci.*, 37, pp. 417–432, 1989.
- <sup>2</sup> A. G. Santo *et al.*, "The MESSENGER Mission to Mercury: Spacecraft and Mission Design." *Planet. Space Sci.*, 49, pp. 1481–1500, 2001.
- <sup>3</sup> C. J. Ercol and A. G. Santo, "Determination of Optimum Thermal Phase Angles at Mercury Perihelion for an Orbiting Spacecraft." 29th International Conference on Environmental Systems, Society of Automotive Engineers, Tech. Paper Ser., paper 1999-01-21123, 10 pp., Denver, CO, July 21–25, 1999.
- <sup>4</sup> C. J. Ercol *et al.*, "Prototype Solar Panel Development and Testing for a Mercury Orbiter Spacecraft." 35th Intersociety Energy Conversion Engineering Conference, American Institute of Aeronautics and Astronautics, paper AIAA-2000-2881, 11 pp., Las Vegas, NV, July 24–28, 2000.
- <sup>5</sup> C. J. Ercol, "MESSENGER Heritage: High-Temperature Technologies for Spacecraft to the Inner Solar System." American Institute of Aeronautics and Astronautics Space 2007 Conference, paper AIAA-2007-6188, 8 pp., Long Beach, CA, September 18–20, 2007.
- <sup>6</sup> P. D. Wienhold and D. F. Persons, "The Development of High-Temperature Composite Solar Array Substrate Panels for the MESSENGER Spacecraft." *SAMPE J.*, 39 (6), pp. 6–17, 2003.
- <sup>7</sup> R. E. Wallis, J. R. Bruzzi, and P. M. Malouf, "Testing of the MESSENGER Spacecraft Phased-Array Antenna." Antenna Measurement Techniques Association 26th Meeting and Symposium, pp. 331–336, Stone Mountain, GA, October 2004.
- <sup>8</sup> C. J. Ercol *et al.*, "Power Subsystem Thermal Design and Early Mission Performance." 4th International Energy Conversion Engineering Conference and Exhibit, paper AIAA-4144, 14 pp., San Diego, CA, June 26–29, 2006.
- <sup>9</sup> R. L. Vaughan *et al.*, "Return to Mercury: The MESSENGER Spacecraft and Mission." Institute of Electrical and Electronics Engineers Aerospace Conference, IEEEAC paper 1562, 15 pp., Big Sky, MT, March 4–11, 2006.
- <sup>10</sup> C. J. Ercol, "Return to Mercury: An Overview of the MESSENGER Spacecraft Thermal Control System Design and Up-to-Date Flight Performance." 38th International Conference on Environmental Systems, SAE International, paper 2008-01-2123, 15 pp., San Francisco, CA, June 29–July 2, 2008.
- <sup>11</sup> C. J. Ercol, G. Dakermanji, and S. C. Laughery, "The MESSENGER Spacecraft Power System: Thermal Performance through the First Mercury Flyby." 6th Annual International Energy Conversion Engineering Conference, paper AIAA-2008-5785, 12 pp., Cleveland, OH, July 28–30, 2008.
- <sup>12</sup> C. J. Ercol, "The MESSENGER Spacecraft Power System: Thermal Performance through Mercury Flyby 3." 8th Annual International Energy Conversion Engineering Conference, paper AIAA-2010-6848, 16 pp., Nashville, TN, July 25–28, 2010.

## CONTACT INFORMATION

To whom correspondence should be addressed: Carl J. Ercol, Lead MESSENGER Thermal Engineer, Space Department, The Johns Hopkins University Applied Physics Laboratory, 11100 Johns Hopkins Road, Laurel, MD 20723-6099.